Supporting Information

Determining Membrane Protein-Lipid Binding Thermodynamics Using Native Mass Spectrometry

Xiao Cong, Yang Liu, Wen Liu, Xiaowen Liang, David H. Russell, and Arthur Laganowsky

Methods

Plasmid construction. The maltose binding protein (MBP) gene from pMAL-C2 (New England Biolabs) amplified by polymerase chain reaction (PCR) and pET28b (Agilent Technologies) linearized with NdeI and XhoI were used in an Infusion (Clonetech) cloning reaction to generate MBP with a thrombin cleavable N-terminal 6xHis-tag. The GlnK gene from *Escherichia coli* was amplified by PCR using genomic DNA as template and cloned into pET28b linearized with NcoI and XhoI using Infusion to generate GlnK with a tobacco etch virus (TEV) protease cleavable N-terminal Strep-tag II tag. The resulting plasmids, pET28-MBP and pET28-GlnK, were confirmed by DNA sequencing.

MBP and GlnK protein expression. The MBP and GlnK expression plasmids were transformed into the *E. coli* Rosetta 2(DE3) pLysS (Agilent Technologies) and *E. coli* ArcticExpress (DE3) RIL (Agilent Technologies), respectively. Several colonies were grown overnight in Terrific Broth (Fisher Scientific) supplemented with either chloramphenicol (45 μg/mL) and kanamycin (50 μg/mL) for MBP or kanamycin (50 μg/mL) for GlnK at 37 ºC. The overnight culture was used to inoculate Terrific Broth (Fisher Scientific) supplemented with kanamycin (50 μg/mL) and grown at 37 ºC until the OD_{600} reached 0.8. The cultures were then chilled on ice prior to adding isopropyl 1-thio-β-D-galactopyranoside (IPTG) to a final concentration of 1 mM and 0.1 mM for MBP and GlnK, respectively. The cells were grown for 24 hours at 20 ºC and harvested by centrifugation at 6000*g* for 10 min, washed once with TBS (20 mM TRIS pH 7.4 at room temperature, 150 mM sodium chloride) and re-pelleted, and pellets stored at -80 °C.

Purification of MBP. Thawed cell pellets expressing MBP were re-suspended in NHA buffer (50 mM TRIS 7.4 at room temperature, 300 mM sodium chloride, 20 mM imidazole, and 10% glycerol). The cells were lysed with 4-5 passes through a Microfluidics M-110P microfluidizer at 20,000 psi and then clarified by centrifugation (30 min at 30,000 *g* at 4 ºC). Unless otherwise stated, all the purification steps were carried out at 4 ºC. The supernatant containing recombinant 6xHis-tagged MBP was purified using a

two-step affinity/desalting method on the AKTAxpress (GE Healthcare). In brief, the clarified supernatant was filtered with a syringe filter before loading onto a HisTrap 5-mL column (GE Healthcare), eluted with the same buffer containing 500 mM imidazole (NHB), peak fraction stored and injected onto a HiPrep 26/10 desalting column (GE Healthcare) equilibrated in NHA buffer with imidazole omitted. The purified 6xHis-tagged MBP was digested with thrombin (3 units of thrombin per mg of protein) overnight at room temperature, concentrated using centrifugal concentrator (Millipore), and loaded onto a HiLoad 16/600 Superdex 75 pg column (GE Healthcare) equilibrated in size-exclusion GF buffer (50 mM TRIS pH 7.4 at room temperature, 100 mM sodium chloride, and 10% glycerol). Peak fractions containing untagged MBP were pooled, concentrated and stored at -80 °C. For native mass spectrometry or SPR analysis, an MBP sample was buffer exchanged into AA buffer (200 mM ammonium acetate buffer pH=7.3 adjusted with ammonium hydroxide) using a centrifugal buffer exchange device (Micro Bio-Spin 6, Bio-Rad) or desalting column (GE Healthcare).

Purification of GlnK. Cell pellets of GlnK were processed and lyzed as described for MBP. The filtered supernatant containing recombinant Strep-tag II-tagged GlnK was then applied onto a StrepTrap HP 5mL column (GE Healthcare) and eluted with the same buffer containing 2.5 mM D-desthiobiotin. The peak fractions containing Strep-tag II-tagged GlnK were pooled, concentrated, and loaded onto a HiLoad 16/600 Superdex 75 pg column (GE Healthcare) equilibrated in GF buffer. The purified Strep-tag II-tagged GlnK was concentrated and stored at -80 °C. GlnK was buffer exchanged into AA buffer for MS experiments as described for MBP.

Preparation of Lysozyme. Hen egg white Lysozyme was dissolved in TBS buffer on ice and buffer exchanged into AA buffer using a centrifugal buffer exchange device (Micro Bio-Spin 6, Bio-Rad).

Expression and purification of ammonia channel (AmtB) wild-type and double mutant. AmtB wild-type and double mutant (N72A/N79A) were expressed and purified as previously described.[1] In brief, the

purified protein was buffer exchanged into AA buffer supplemented with 0.5% tetraethylene glycol monooctyl ether (C_8E_4) for native mass spectrometry experiments.

Protein quantification. Soluble and membrane protein concentration was determined with the *DC* Protein Assay kit (Bio-Rad) using bovine serum albumin as the standard.

Preparation and titration of ligands or phospholipids. D-(+)-Maltose, maltotriose, *N, N′, N″*-triacetylchitotriose (NAG3) and adenosine 5′-diphosphate (ADP) were dissolved in AA buffer. For phospholipid such as 1-palmitoyl-2-oleoyl-*sn*-glycero-3-phospho-(1'-*rac*-glycerol) (POPG), 1-palmitoyl-2-oleoyl-*sn*-glycero-3-phosphoethanolamine (POPE), 1-palmitoyl-2-oleoyl-*sn*-glycero-3-phosphate (POPA), 1-palmitoyl-2-oleoyl-*sn*-glycero-3-phospho-L-serine (POPS), 1,1',2,2'-tetraoleoyl-cardiolipin (TOCDL), 1,2-dilauroyl-*sn*-glycero-3-phospho-(1'-*rac*-glycerol) (DLPG), 1,2-dimyristoyl-*sn*-glycero-3-phospho-(1'-rac-glycerol) (DMPG), and 1,2-dipalmitoyl-*sn*-glycero-3-phospho-(1'-*rac*-glycerol) (DPPG) (Avanti Polar Lipids Inc., Alabama, USA), stock solution of each lipid were prepared in AA buffer supplemented with 0.5% C_8E_4 and 5 mM 2-mercaptoethanol (β-ME) as described previously.[2] Phospholipid concentration was determined by phosphorus analysis.[3,4] For each ligand, a serial dilution was performed to make sets of solutions containing different concentrations of ligands and 1.2 μL of ligand solution was then mixed with 1.2 μL of freshly-prepared protein solution. The protein ligand mixture was then loaded into a gold-coated capillary tip, followed by equilibration in the source chamber of the mass spectrometer set at a given temperature for ~10 min before recording mass spectra. Notably, we did not observe a change in mole fractions of apo or ligand-bound proteins with longer incubation time (Figure S7).

Design and construction of the apparatus to control temperature. A general description of the apparatus is provided in the main text (Figure 1A and Figure S1). In more detail, two 120 mm central processing unit (CPU) fans (Antec-TriCool) were fixed to the source chamber to direct the external air into the

chamber passing over a heat sink (40 x 40 x 14.5 mm, Advanced Thermal Solutions) attached to a Peltier thermoelectric chip (40 x 40 x 3.5 mm, 12V 5A, Adafruit Industries). The thermoelectric chip is powered by a direct current (DC) power supply and the applied voltage is adjusted to heat the incoming external airflow to a desired temperature. A small T-type thermocouple (0.23 mm O.D. IT-24P, Physitemp Instruments) connected to an USB-TC01 thermocouple measurement device (National Instruments) was used to digitally record the temperature. The small thermocouple could be inserted directly into ~2 μL of sample solution within the gold-coated capillary used for nano-electrospray ionization (nESI) to monitor sample temperature (T_{sample}). The equilibrium of T_{sample} is reached within ~40 seconds after moving the nESI stage into the source chamber and the temperature holding within ±0.3 °C (Figure S1B). A calibration curve was generated for T_{sample} as a function of source air temperature (T_{air}) (Figure S1C), which enabled us to set a desired T_{sample} while monitoring T_{air} to avoid potential cross contamination by re-insertion of the delicate thermocouple probe into the next sample. An insulating barrier was inserted into the source chamber to direct airflow and prevent heat transfer from the source, which is heated in our experiments. The insulating barrier was made of cardboard. Generally, the capillary used for nESI spray is about 2.5 cm long with an inner I.D. of ~1 mm. at the base and 0.04 mm at the tip. The liquid volume in our experiments is usually ~2 μL resulting in a liquid column inside the capillary on the order of 0.25 cm in length. As the whole capillary is incubated in the source chamber of the mass spectrometer at set temperature, and given the liquid column is so short, the temperature gradient is so little that it can be considered negligible.

Native mass spectrometry (MS) analysis. Native MS was performed on a Synapt G1 HDMS instrument (Waters corporation) with a 32k RF generator. For soluble protein-ligand systems, the instrument was set to a source pressure of 6.2-6.4 mbar, capillary voltage of 1.4 kV, sampling cone voltage of 20 V, extractor cone voltage of 3.0 V, trap collision voltage of 20 V, collision gas (Argon) flow rate of 4 ml/min (3.6 x 10^{-2} mbar), and T-wave settings (velocity/height) for trap, IMS and transfer of 100 ms^{-1}/0.5 V,100 ms^{-1}/4.0 V, and 100 ms^{-1}/3.0 V, respectively. The source temperature (50 ^{o}C) and trap bias (22 V) were

optimized for soluble proteins. For membrane protein-lipid binding systems, these instrument parameters were tuned to maximize ion intensity but simultaneously preserve the native-like state of AmtB (Figure S5). The instrument was set to a capillary voltage of 1.7 kV, sampling cone voltage of 200 V, extractor cone voltage of 10 V and argon flow rate at 7 ml/min (5.2 x 10^{-2} mbar). The T-wave settings for trap (300 ms^{-1}/2.0 V), IMS (300 ms^{-1}/20 V) and transfer (100 ms^{-1}/10 V), source temperature (90 ^{o}C) and trap bias (35 V) were also optimized.

Surface plasmon resonance (SPR) analysis of protein-ligand interactions. SPR experiments were performed using the Biacore 3000 optical biosensor with research-grade CM5 sensor chips (GE Healthcare/Biacore AB, Uppsala, Sweden). Sensor surfaces were prepared at 25 ˚C using amine-coupling kits (GE Healthcare/Biacore AB) at a flow rate of 5 µl/min in PBS (10 mM sodium phosphate pH 7.4, 150 mM sodium chloride). Lysozyme surface was prepared using standard procedures; the flow cell was activated with 35 µl of a 1:1 mixture of 0.4 M EDC and 0.1 M NHS, followed by injection of 5 µg/ml lysozyme (in 10 mM sodium acetate, pH 5.5) until surface density reached ~2000 RU, and finally the lysozyme coupled surface was deactivated with 1.0 M ethanolamine (pH 8.5) for 5 min. In order to immobilize enough MBP, a minor modification was made when preparing the sensor surface: after 10 min activation followed by injection of MBP solution (50 µg/ml in 10 mM sodium acetate, pH 4.0), deactivation was achieved by 10 injections (1 min at 50 µl/min) of AA buffer and 5 injections of 100 µM maltotriose (in AA buffer) until the MBP surface was stable. Two surfaces (with slight differences in density) were created for each protein and one flow cell without protein coupled was used as a reference to subtract out systematic noise.

SPR response data were collected for the soluble molecules binding to the protein surfaces at 25, 29, 33, and 37 ˚C. At each temperature, samples prepared by serial dilution (factor of 3, in duplicate) in running AA buffer were injected over the protein and reference surfaces for 30 seconds at a flow rate of 50 µl/min. Data eveluation was performed by calculating binding response (R_{eq}, average response of 5

seconds during equilibrium phase) for each injection and plotted as a function of ligand concentration (A). The equilibrium dissociation constant (K_D) was obtained by fitting a single site binding curve to the data using equation: $R_{eq} = R_{max} \times A / (K_D + A)$, where R_{max} is the maximum response when the active surface is saturated. Binding thermodynamic constants for each compound were calculated from the K_D values measured by SPR at different temperatures and subjected to van't Hoff analysis.

Isothermal titration calorimetry (ITC) analysis of the interactions. ITC experiments were carried out using the MicroCal VP-ITC instrument at 29 ˚C in AA buffer. For each experiment, 10 µl (5 µL for the first injection) of either 500 µM maltose, 450 µM maltotriose or 2 mM NAG3 was injected into 40 µM MBP or 200 µM lysozyme. Each injection (at a speed of 0.5 µl/s) was spaced with 300 s intervals and set to a stirring speed of 300 rpm. ITC data were background subtracted with data collected for ligands injected into AA buffer. The titration data were integrated and fit to a one-site binding model using MicroCal Origin software (version 5.0).

Native MS data analysis. Native MS data was processed using the software program Pulsar[5] and deconvoluted using Unidec.[6] The intensities of protein (P) and protein-ligand (PL) species were converted to mole fraction for a given ligand titration. The interaction between P and PL is dependent on the apparent equilibrium association constant (K_A). For soluble protein systems, we applied the following sequential binding model. For protein binding to one ligand:

$$\mathbf{P + L} \overset{\mathbf{K_A}}{\Leftrightarrow} \mathbf{PL} \quad \mathbf{K_A} = \frac{\mathbf{[PL]}}{\mathbf{[P][L]}} \qquad \mathbf{(1)}$$

Or binding to multiple ligands:

$$\mathbf{PL_{n-1} + L} \overset{\mathbf{K_{An}}}{\Leftrightarrow} \mathbf{PL_n} \quad \mathbf{K_{An}} = \frac{\mathbf{[PL_n]}}{\mathbf{[PL_{n-1}][L]}} \qquad \mathbf{(2)}$$

where n is the number of bound ligands, and K_{An} is the equilibrium association constant for the n_{th} ligand binding to the protein. $[P]_{total}$ represents total protein concentration added:

$$\mathbf{[P]_{total}} = \mathbf{[P]} + \sum_{i=1}^{n}\mathbf{[PL}_i\mathbf{]} = \mathbf{[P]} + \sum_{i=1}^{n}\mathbf{[P][L]}^i \prod_{j=1}^{i}\mathbf{K_{Aj}} \qquad \mathbf{(3)}$$

Equation (2) can be rearranged to calculate the mole fraction (F_n) of PL_n:

$$\mathbf{F_n = \frac{[PL_n]}{[P]_{total}} = \frac{[L]^n \prod_{j=1}^{n} K_{Aj}}{1+\sum_{i=1}^{n}[L]^i \prod_{j=1}^{i} K_{Aj}}} \quad \mathbf{(4)}$$

where [L] is the free ligand concentration at equilibrium. The free ligand can be calculated if the concentration of protein is known as follows:

$$\mathbf{[L] = [L]_{total} - [P]_{total} \cdot \sum_{i=1}^{n} iF_i} \quad \mathbf{(5)}$$

To obtain K_{An}, the sequential binding model was globally fit to mole fraction data collected at a given temperature through minimization of the pseudo-χ^2 function:[7]

$$\chi^2 = \sum_{i=0}^{n}\sum_{j=1}^{d}\left(F_{i,j,exp} - F_{i,j,calc}\right)^2 \quad \mathbf{(6)}$$

where *n* is the number of bound ligands and *d* is the number of the experimental mole fraction data points. Van't Hoff analysis,[8] plot of the natural logarithm of K_{An} as a function of the reciprocal of temperature, were generated to determine the enthalpy change (ΔH), entropy change (-TΔS) and the Gibbs free energy of the binding (ΔG) based on equation:

$$\mathbf{\ln K_A = \frac{-\Delta G}{RT} = \frac{T\Delta S - \Delta H}{RT} = -\frac{\Delta H}{R}\cdot\frac{1}{T} + \frac{\Delta S}{R}} \quad \mathbf{(7)}$$

For membrane protein-lipid binding systems, we took into account that lipids readily associate as evident in some mass spectra (Figure S8), which would alter the lipid concentration available for binding. For lipid self-assemble:

$$\mathbf{L + L \overset{K_{AGG1}}{\Longleftrightarrow} L_2 \quad K_{AGG1} = \frac{[L_2]}{[L]_{avail}^2}} \quad \mathbf{(8)}$$

$$\mathbf{L_{n-1} + L \overset{K_{AGG(n-1)}}{\Longleftrightarrow} L_n \quad K_{AGG(n-1)} = \frac{[L_n]}{[L_{n-1}][L]_{avail}}} \quad \mathbf{(9)}$$

where $[L]_{avail}$ is the concentration of lipids 'free' to bind proteins and $K_{AGG(n-1)}$ is the equilibrium association constant for the lipid aggregate (L_{n-1}) to bind another lipid to form L_n. Thus,

$$\mathbf{[L]_{total} = [L]_{avail} + \sum_{i=2}^{n} i[L]_{avail}^{i} \prod_{j=2}^{i} K_{AGG(j-1)}} \quad \mathbf{(10)}$$

Although we observe lipid aggregates in the mass spectrum, it is difficult to quantify these species due to a mixture of states including those bound to adduct, such as the C_8E_4 detergent (Figure S8A). We

therefore made the assumption that K_{AGG} for each binding is equal and used this model with an *n* of 2, which simplifies equation (10) to:

$$[\mathbf{L}]_{\mathbf{total}} = [\mathbf{L}]_{\mathbf{avail}} + \mathbf{2K_{AGG}}[\mathbf{L}]^{\mathbf{2}}_{\mathbf{avail}} \quad \textbf{(11)}$$

L_{avail} can be solved and taking the positive solution:

$$[\mathbf{L}]_{\mathbf{avail}} = \frac{-1+\sqrt{1+8\mathbf{K_{AGG}}[\mathbf{L}]_{\mathbf{total}}}}{4\mathbf{K_{AGG}}} \quad \textbf{(12)}$$

Incorporating this lipid self-association model introduces one additional fitting parameter and essentially divides the total lipid into a fraction 'free' to bind and a fraction that cannot bind. In comparison to the sequential binding model, the lipid-binding model resulted in better fit (Figure S8) that was statistically justified (F-test, $p < 0.001$). Therefore, this model was applied to determine K_{An} for each lipid-binding event. Although other more sophisticated models could be considered, such as including protein-detergent or lipid-detergent interactions, we observed using our sequential lipid-binding model similar K_{An} values (within experimental error) when varying either protein or detergent concentrations. Therefore, we opted for the simplest model to describe our experimental data.

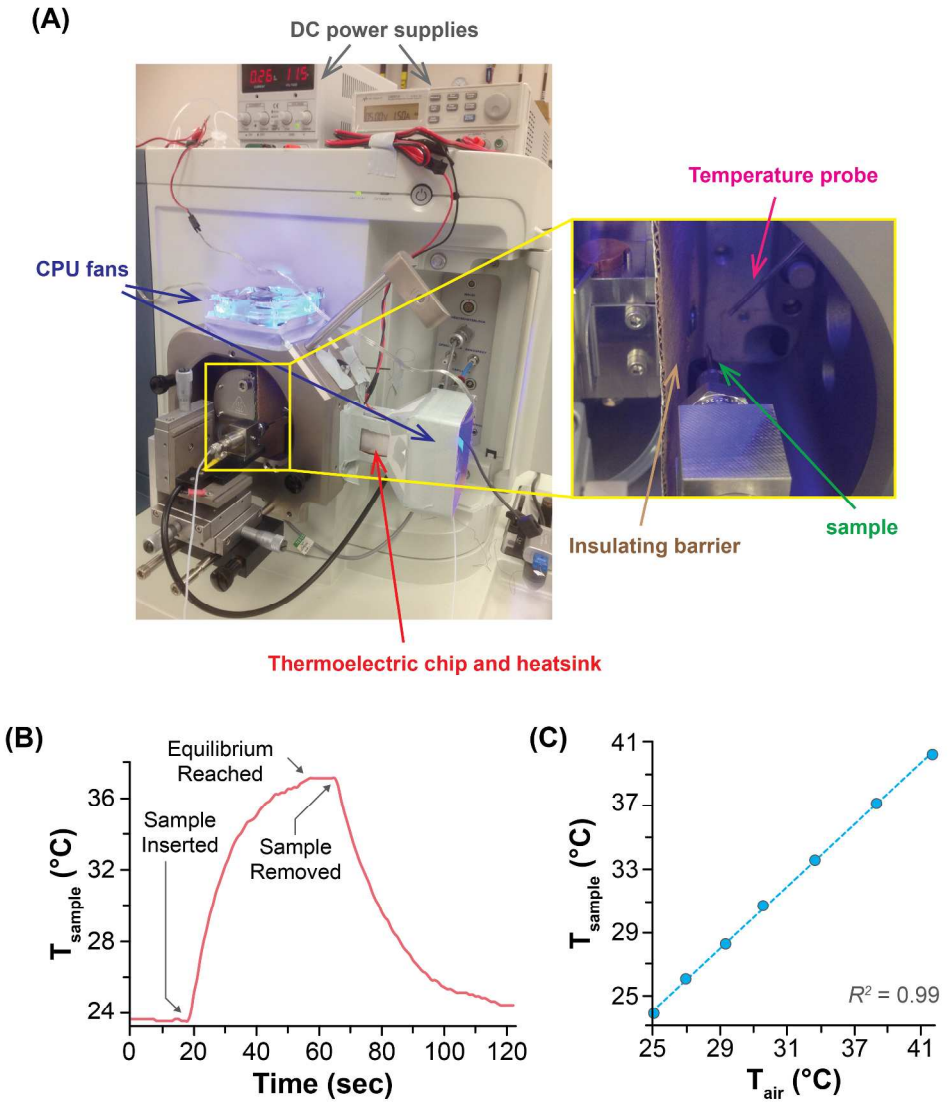

Figure S1. (A) Photographs of the setup to control temperature of sample. Additional details regarding the construction of this device can be found in "Supporting Methods". **(B)** Plot of T_{sample} when moving the nano-electrospray stage into and out of the source chamber. **(C)** Calibration curve for T_{sample} as a function of T_{air}.

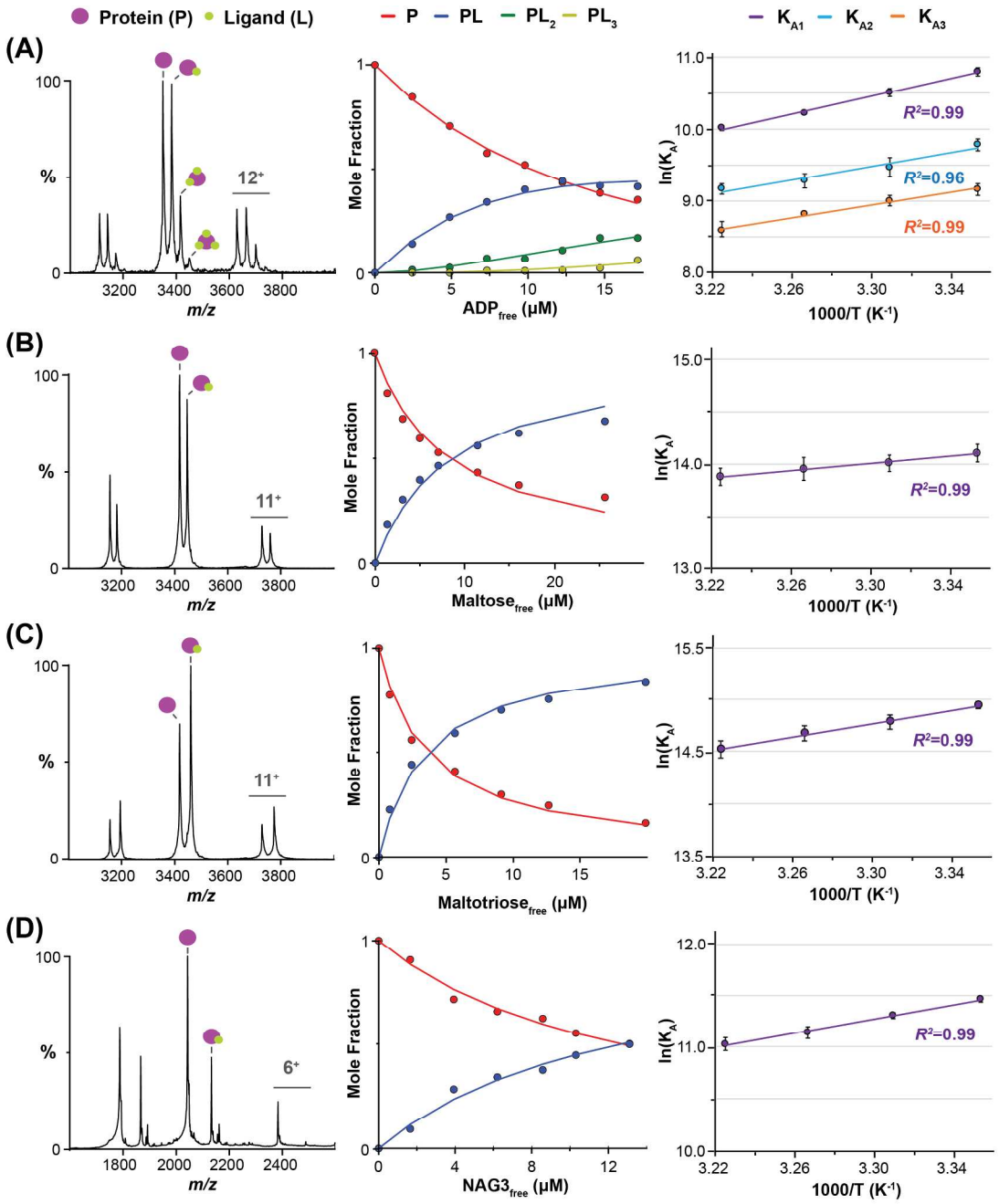

Figure S2. Soluble protein-ligand binding thermodynamics determined by native MS. Shown are representative mass spectra (left panel), plots of mole fraction of apo (P) and ligand-bound (PL_n) protein as a function of free ligand concentration collected at 29 ^oC (middle panel), and Van't Hoff plots (right panel) for **(A)** GlnK binding ADP_{1-3} molecules, MBP binding maltose **(B)** or maltotriose **(C)**, and **(D)** lysozyme binding NAG3. Reported for Van't Hoff plots are the mean and standard deviation (n = 3).

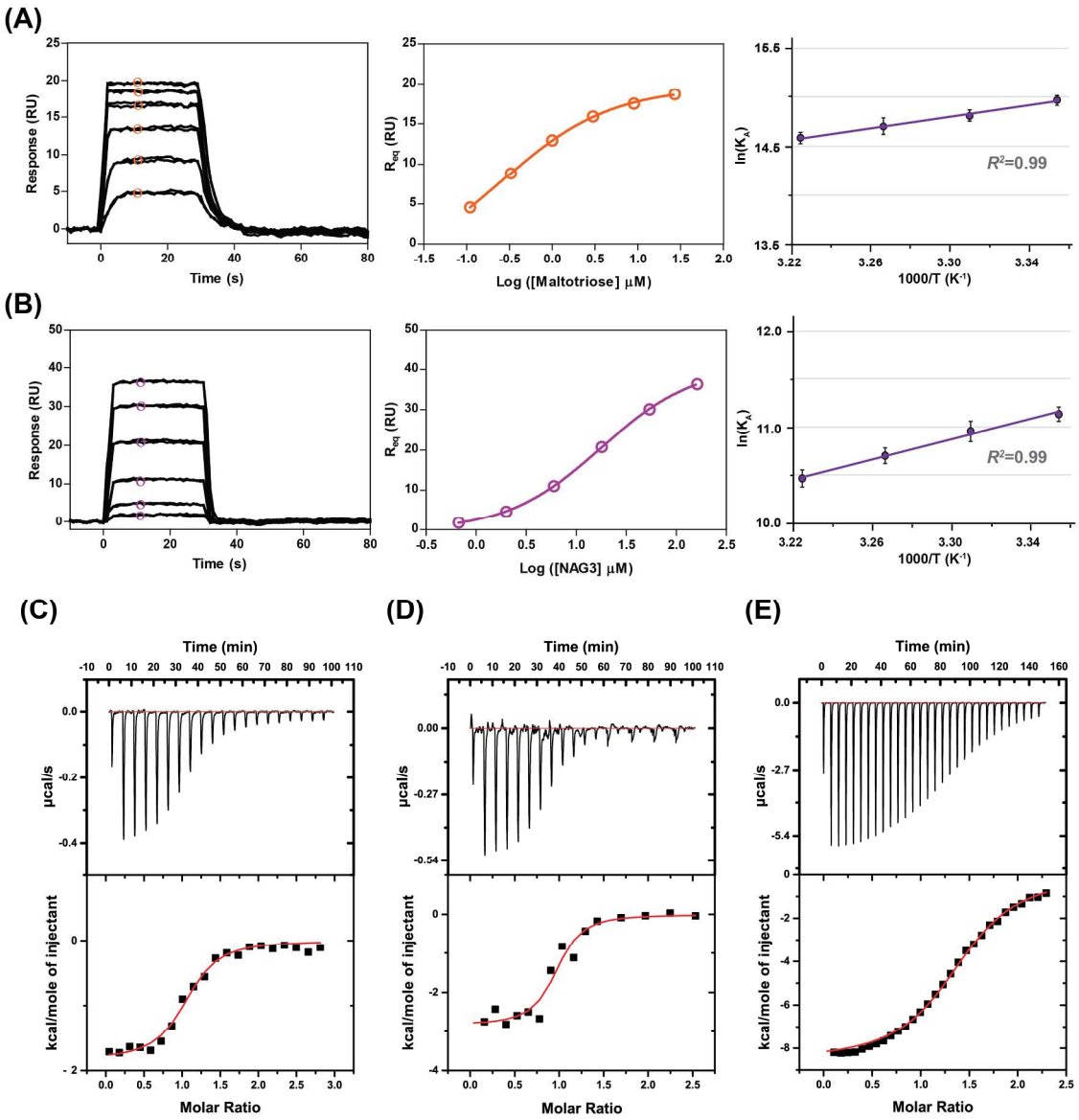

Figure S3. SPR and ITC of soluble protein-ligand systems. The representative binding and dissociation SPR profiles (in duplicate) (left panel), binding curves at 29 °C (the average binding response during equilibrium phase as a function of the concentration of injected molecules) (middle panel) and Van't Hoff plots (right panel) for **(A)** MBP-maltotriose and **(B)** lysozyme-NAG3 binding**.** ITC baseline-corrected power-versus-time plot for the titration (top panel) and integrated heats plotted over molar ratio (bottom panel) for **(C)** MBP-maltose, **(D)** MBP-maltotriose, and **(E)** lysozyme-NAG3 binding.

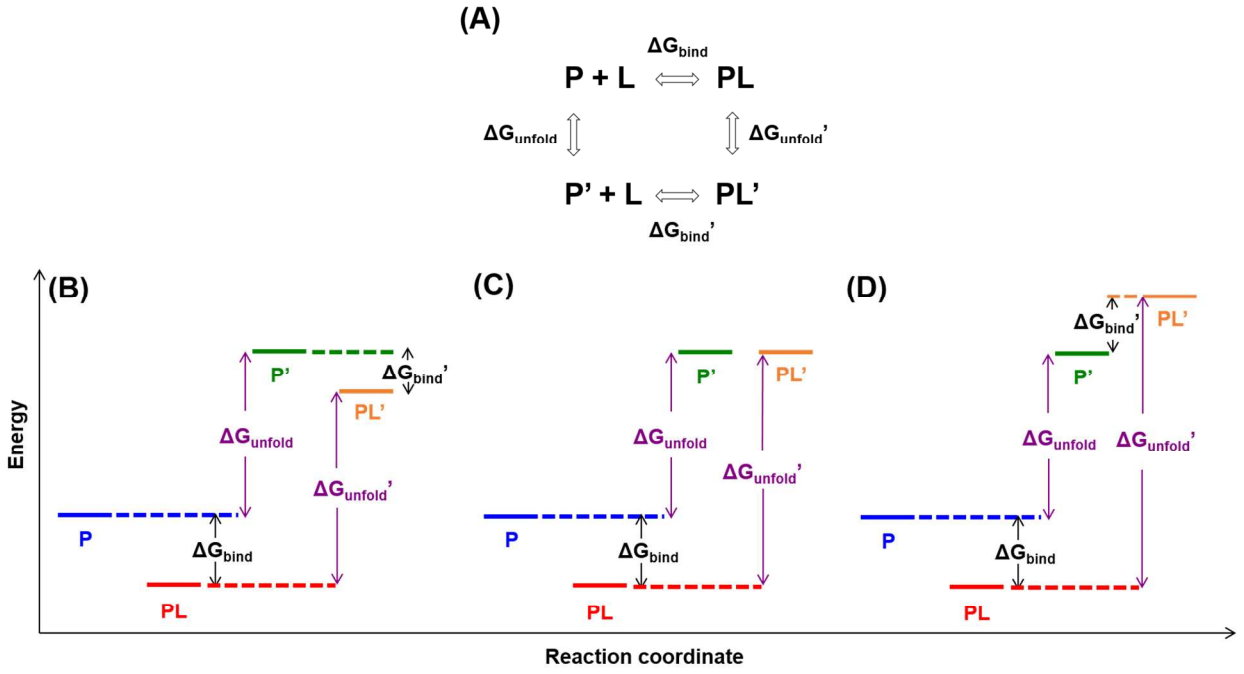

Figure S4. Difference in stabilization versus binding energies. **(A)** Scheme showing the equilibrium of protein (P) binding lipid or ligand (L) and unfolding. The (') denotes a partially or fully unfolded protein. ΔG_{bind} (or ΔG_{bind}') represent the Gibbs free energy of binding reactions between lipids and native (or unfolded) protein. ΔG_{unfold} (or ΔG_{unfold}') represent the Gibbs free energy of unfolding process of apo or lipid-bound protein. **(B-D)** Hypothetical energy diagrams of possible scenarios that could occur in gas-phase and solution unfolding experiments. The unfolded protein-lipid complex can be **(B)** lower, **(C)** same, or **(D)** higher in energy. In general, the stabilization energy ($\Delta\Delta G$) is not equal to the binding energy (ΔG_{bind}) and influenced by how unfolded lipid binding modulates protein structure.

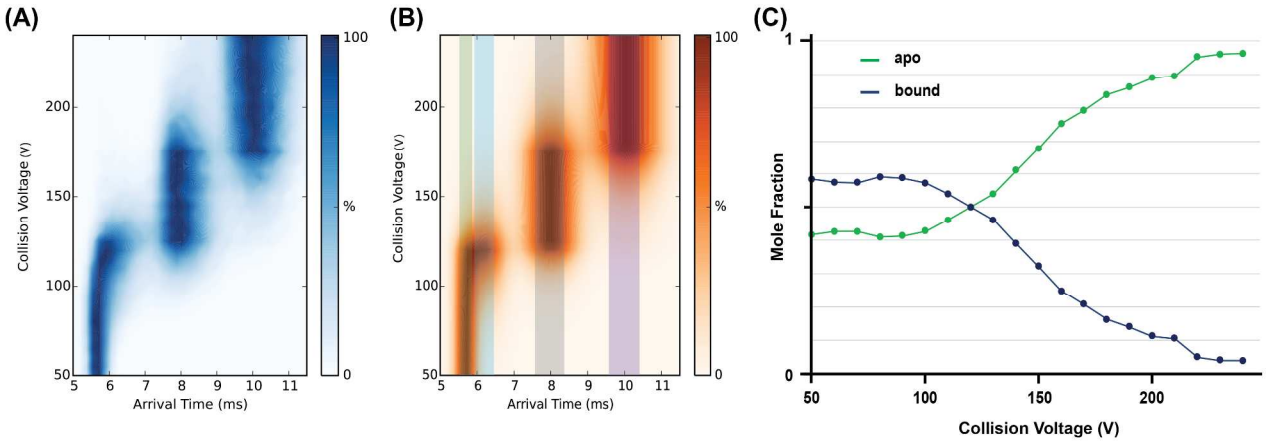

Figure S5. Optimization of native mass spectrometry (MS) settings for membrane proteins. **(A)** Experimental and **(B)** modeled[1] gas-phase unfolding plots of 15^{+} ion of ammonia channel (AmtB) (fitting $\chi^2 = 2.96$). Extraction regions for native-like (green) and the first (blue), second (grey) and third (purple) partially unfolded states are shown. **(C)** Plot of the mole fraction of apo and lipid-bound AmtB as a function of collision voltage for 1.5 μM AmtB mixed with 16.7 μM POPE. A collision voltage of 60 V was selected for native MS experiments where the native-like state of AmtB is preserved.

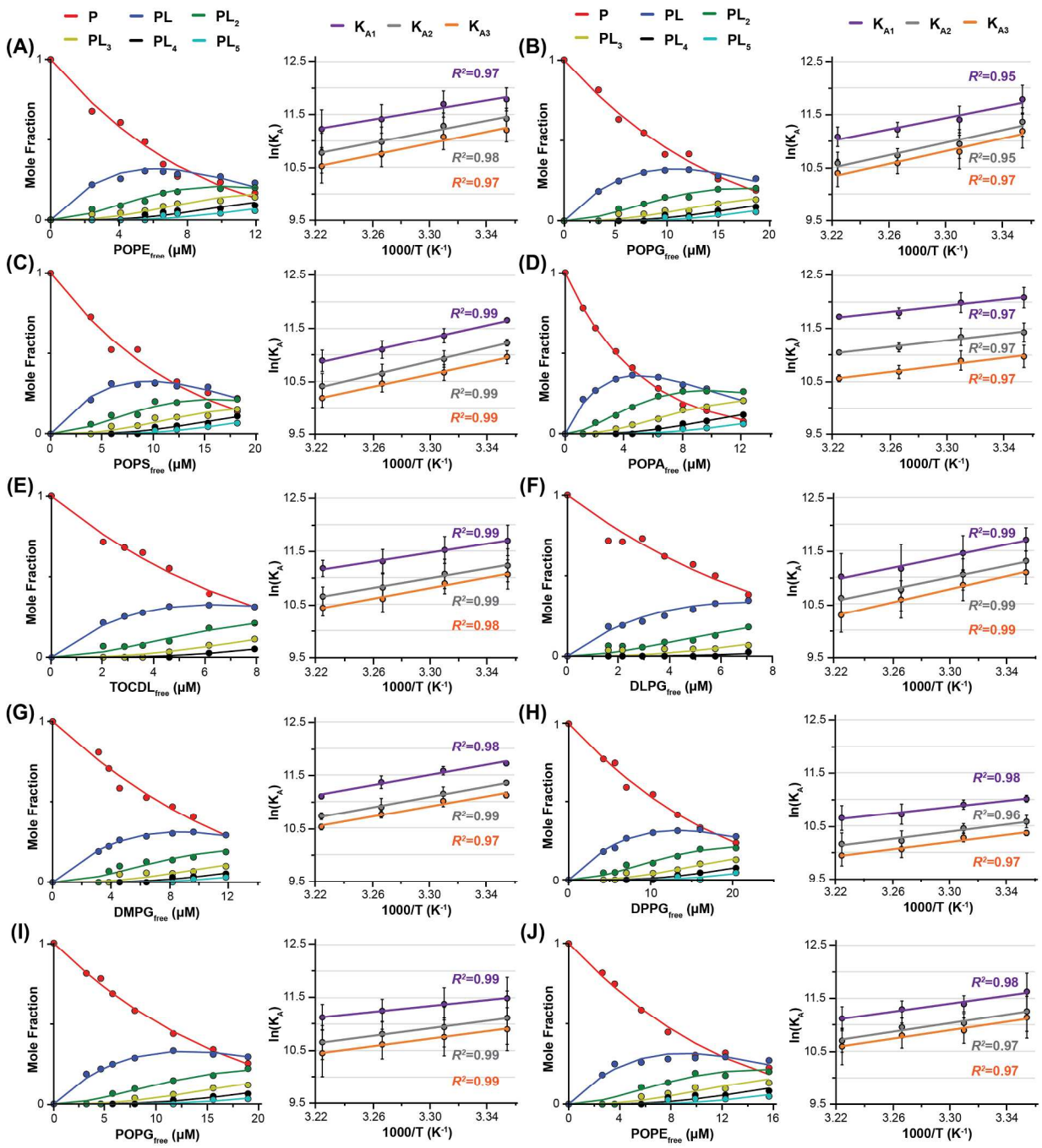

Figure S6. Membrane protein-lipid binding thermodynamics by native MS. Representative plots of mole fractions of apo (P) and lipid-bound (PL_n) AmtB collected at 29 ^oC (left panel) and Van't Hoff plots (right panel). AmtB binding to **(A)** POPE, **(B)** POPG, **(C)** POPS, **(D)** POPA, **(E)** TOCDL, **(F)** DLPG, **(G)** DMPG, and **(H)** DPPG. $AmtB^{N72AN79A}$ binding to **(I)** POPG and **(J)** POPE. For Van't Hoff plots, reported are the mean and standard deviation (n = 3).

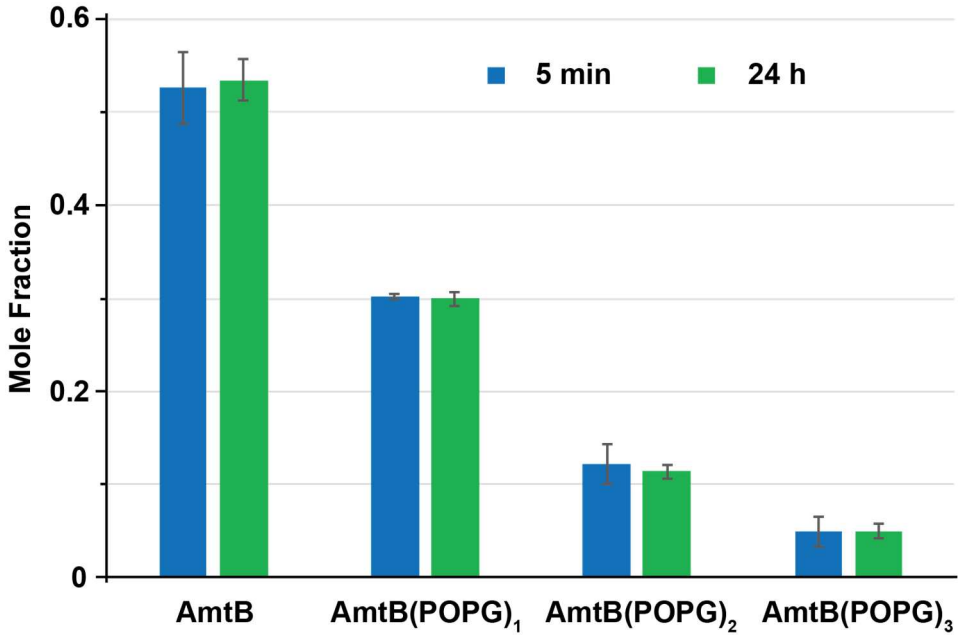

Figure S7. Mole fraction of membrane protein-lipid complexes incubated for 5 min or 24 h. Shown is data for 1.5 μM AmtB mixed with 10 μM POPG at T_{sample} = 25 °C for 5 min in the mass spectrometer or 24 hours in a thermal cycler set at 25 °C. Reported is the mean and standard deviation from repeated measurements using different gold-coated capillary tips (n = 3).

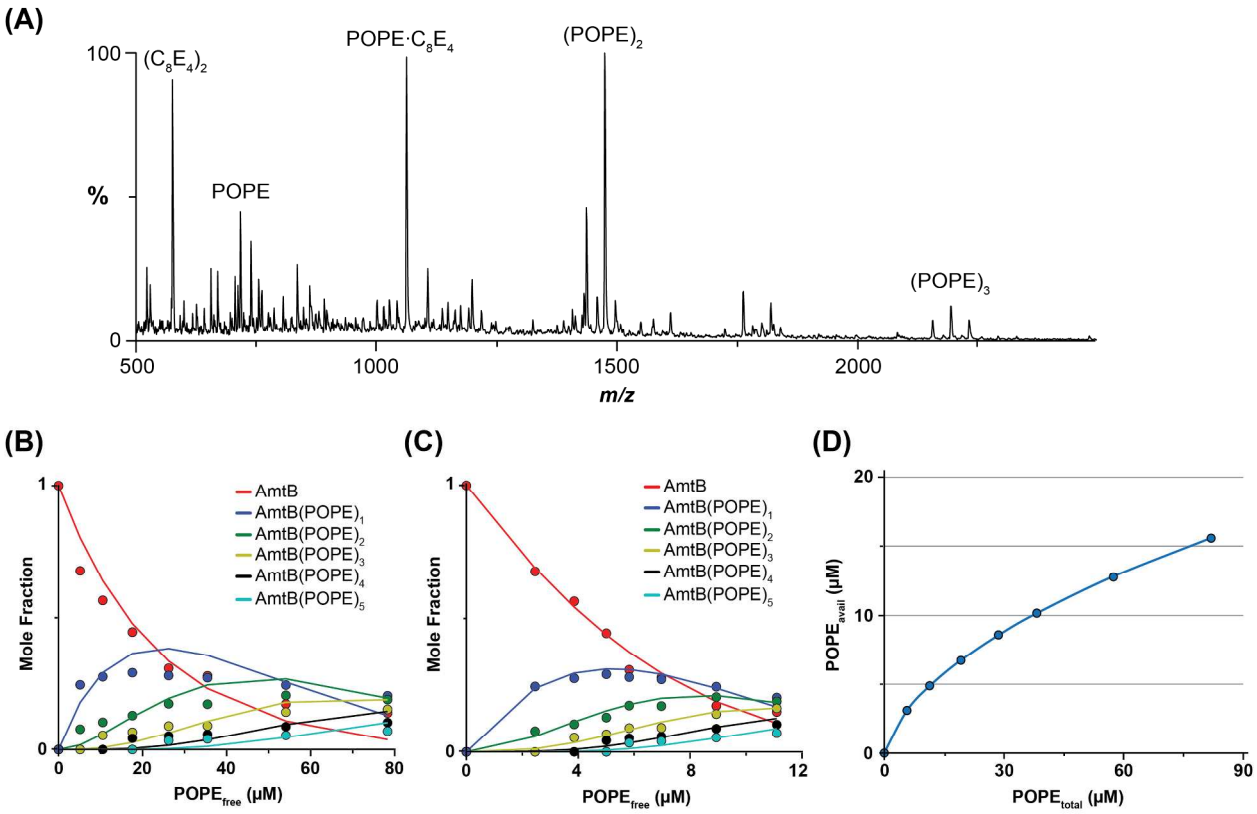

Figure S8. Membrane protein-lipid binding data fit to different binding models. **(A)** Representative mass spectrum showing POPE self-assembly and POPE-detergent complexes. **(B-C)** Plots of mole fraction AmtB(POPE)$_{0\text{-}5}$ determined from the titration series of POPE (dots) and resulting fit (solid lines) using a **(B)** sequential binding model (R^2 = 0.96, χ^2 = 0.112) or **(C)** modified sequential lipid-binding model (R^2 = 0.99, χ^2 = 0.0198). **(D)** Plot of available POPE concentrations calculated by Equation 12 in "Supporting Methods" as a function of total POPE concentrations titrated. K_{AGG} applied is abstracted from fitted data in **(C)** using a modified sequential lipid-binding model, which in this example equals 7.26 μM.

Table S1. Binding affinities of soluble protein-ligand systems by native MS. Reported for each temperature (T) is the mean and standard deviation for K_D obtained from fitting a sequential binding model to a mass spectra dilution series, typically 7-9 dilutions (n = 3).

Protein	Ligand	T (K)	K_{D1} (μM)	K_{D2} (μM)	K_{D3} (μM)	R^2	χ^2
MBP	maltose	298	0.75 ± 0.06	--	--	0.98	0.025
		302	0.83 ± 0.06			0.98	0.026
		306	0.87 ± 0.09			0.99	0.021
		310	0.94 ± 0.08			0.99	0.019
	maltotriose	298	0.32 ± 0.01	--	--	0.99	0.013
		302	0.38 ± 0.03			0.99	0.006
		306	0.43 ± 0.03			0.99	0.007
		310	0.50 ± 0.04			0.99	0.008
lysozyme	NAG3	298	10.5 ± 0.27	--	--	0.96	0.055
		302	12.3 ± 0.36			0.96	0.052
		306	14.5 ± 0.81			0.96	0.047
		310	16.3 ± 1.01			0.98	0.027
GlnK	ADP	298	20.4 ± 1.15	56.3 ± 4.57	105 ± 8.28	0.99	0.011
		302	27.2 ± 1.53	77.0 ± 9.75	123 ± 8.74	0.99	0.007
		306	36.3 ± 0.31	92.8 ± 9.19	150 ± 33.3	0.99	0.006
		310	44.5 ± 1.55	104 ± 7.90	167 ± 35.8	0.99	0.011

Table S2. Binding affinities of soluble protein-ligand systems by SPR and ITC. Reported for SPR is the mean and standard deviation (n = 3) at each temperature (T) and results for ITC (n = 1) at 302 K.

Protein	Ligand	T (K)	SPR	ITC
			K_{D1} (μM)	K_{D1} (μM)
MBP	maltose	298	--	--
		302	--	1.82
		306	--	--
		310	--	--
	maltotriose	298	0.32 ± 0.02	--
		302	0.37 ± 0.02	0.87
		306	0.41 ± 0.03	--
		310	0.47 ± 0.03	--
lysozyme	NAG3	298	14.7 ± 1.05	--
		302	17.6 ± 1.76	14.4
		306	22.5 ± 1.80	--
		310	28.6 ± 2.48	--

Table S3. Thermodynamic parameters for soluble protein-ligand binding by native MS, SPR, and ITC. Reported for MS and SPR is the mean and standard deviation (n = 3) and results for ITC (n = 1). The reported ΔG at 298K is calculated using ΔH and -TΔS.

Protein	Ligand	ΔH (kJ/mol)		
		MS	SPR	ITC
MBP	maltose	-14.1 ± 0.89	--	-7.69 ± 0.22
	maltotriose	-26.5 ± 1.30	-23.9 ± 1.21	-11.9 ± 0.70
lysozyme	NAG3	-28.4 ± 1.43	-43.2 ± 2.49	-35.8 ± 0.65
GlnK	ADP	-50.6 ± 2.52	--	--
		-39.2 ± 5.60		
		-36.6 ± 2.43		

Protein	Ligand	-TΔS (298K) (kJ/mol)		
		MS	SPR	ITC
MBP	maltose	-20.8 ± 0.87	--	-25.2
	maltotriose	-10.5 ± 1.26	-13.1 ± 1.19	-22.9
lysozyme	NAG3	-0.01 ± 1.40	15.6 ± 2.45	7.70
GlnK	ADP	23.9 ± 2.48	--	--
		15.0 ± 5.50		
		13.8 ± 2.38		

Protein	Ligand	ΔG (298K) (kJ/mol)		
		MS	SPR	ITC
MBP	maltose	-34.9 ± 1.76	--	-32.9 ± 0.22
	maltotriose	-37.0 ± 2.56	-37.0 ± 2.40	-34.8 ± 0.70
lysozyme	NAG3	-28.4 ± 2.83	-27.6 ± 4.94	-28.1 ± 0.65
GlnK	ADP	-26.7 ± 5.00	--	--
		-24.2 ± 11.1		
		-22.8 ± 4.81		

Table S4. Binding affinities for AmtB binding lipids. Reported as described in Table S1 with the exception that a lipid-binding model was used.

Lipid	T (K)	Ammonia channel protein (AmtB)			R^2	χ^2
		K_{D1} (μM)	K_{D2} (μM)	K_{D3} (μM)		
POPE	298	7.73 ± 1.71	11.1 ± 2.34	13.8 ± 3.28	0.99	0.020
	302	8.51 ± 2.14	12.8 ± 3.19	15.7 ± 4.01	0.99	0.018
	306	11.3 ± 3.23	17.5 ± 5.31	21.7 ± 5.57	0.99	0.016
	310	13.9 ± 5.27	22.0 ± 8.90	27.8 ± 9.41	0.99	0.015
POPG	298	7.75 ± 1.90	11.9 ± 3.06	14.3 ± 4.42	0.99	0.028
	302	11.3 ± 2.75	18.1 ± 4.76	21.2 ± 6.38	0.99	0.021
	306	13.5 ± 1.87	22.0 ± 2.72	25.8 ± 4.96	0.99	0.016
	310	15.6 ± 2.75	25.9 ± 5.19	31.3 ± 7.41	0.99	0.021
POPS	298	8.68 ± 0.24	13.3 ± 0.88	17.5 ± 2.12	0.99	0.027
	302	11.7 ± 1.54	18.2 ± 2.73	23.4 ± 3.30	0.99	0.017
	306	15.3 ± 2.54	23.9 ± 4.0	28.9 ± 4.38	0.99	0.010
	310	18.8 ± 3.56	30.7 ± 7.01	37.8 ± 6.70	0.99	0.015
POPA	298	5.70 ± 1.05	11.0 ± 1.89	17.4 ± 3.47	0.99	0.008
	302	6.28 ± 1.10	11.9 ± 1.94	18.7 ± 3.15	0.99	0.007
	306	7.54 ± 0.72	14.5 ± 1.19	23.0 ± 2.69	0.99	0.009
	310	8.10 ± 0.31	15.9 ± 0.23	25.9 ± 1.65	0.99	0.014
TOCDL	298	8.53 ± 2.50	13.7 ± 4.24	16.1 ± 4.48	0.99	0.008
	302	10.1 ± 2.62	16.0 ± 4.45	18.8 ± 3.80	0.99	0.006
	306	12.5 ± 2.85	20.5 ± 5.51	25.5 ± 6.82	0.99	0.005
	310	14.1 ± 2.20	24.0 ± 4.44	29.6 ± 5.09	0.99	0.007
DLPG	298	8.35 ± 1.77	12.4 ± 2.36	15.5 ± 3.37	0.97	0.053
	302	11.0 ± 3.30	16.3 ± 4.40	19.9 ± 5.23	0.98	0.038
	306	15.1 ± 5.78	22.2 ± 7.66	26.4 ± 8.20	0.98	0.036
	310	17.4 ± 6.30	25.7 ± 8.41	35.3 ± 11.0	0.99	0.020
DMPG	298	8.14 ± 0.30	11.8 ± 0.39	14.8 ± 0.76	0.99	0.021
	302	9.34 ± 0.74	14.5 ± 1.82	16.5 ± 1.83	0.99	0.012
	306	11.7 ± 1.30	18.7 ± 3.12	21.3 ± 1.39	0.99	0.014
	310	15.2 ± 0.61	22.0 ± 1.38	27.0 ± 1.48	0.99	0.013
DPPG	298	16.5 ± 1.05	25.6 ± 3.06	31.6 ± 1.52	0.90	0.020
	302	18.5 ± 1.68	28.9 ± 2.45	34.6 ± 2.63	0.99	0.012
	306	22.3 ± 4.07	36.8 ± 6.35	43.1 ± 6.34	0.99	0.013
	310	24.1 ± 5.23	39.2 ± 7.74	48.6 ± 9.01	0.99	0.014

Table S5. Thermodynamic parameters for AmtB binding lipids. Reported as described in Table S3.

Lipid		Ammonia channel protein (AmtB)		
		ΔH (kJ/mol)	-TΔS (298K) (kJ/mol)	ΔG (298K) (kJ/mol)
POPE	K_{A1}	-37.4 ± 4.99	8.05 ± 4.88	-29.3 ± 9.87
	K_{A2}	-43.1 ± 4.53	14.7 ± 4.43	-28.4 ± 8.96
	K_{A3}	-45.7 ± 5.27	17.8 ± 5.18	-27.9 ± 10.5
POPG	K_{A1}	-44.7 ± 7.27	15.6 ± 7.11	-29.1 ± 14.4
	K_{A2}	-49.4 ± 7.91	21.4 ± 7.75	-28.0 ± 15.7
	K_{A3}	-50.2 ± 6.25	22.6 ± 6.12	-27.6 ± 12.4
POPS	K_{A1}	-49.1 ± 2.22	20.2 ± 2.18	-28.9 ± 4.40
	K_{A2}	-52.6 ± 1.72	24.8 ± 1.68	-27.8 ± 3.40
	K_{A3}	-48.0 ± 1.94	20.9 ± 1.91	-27.2 ± 3.85
POPA	K_{A1}	-24.6 ± 2.90	-5.35 ± 2.85	-30.0 ± 5.75
	K_{A2}	-25.6 ± 3.09	-2.82 ± 3.02	-28.4 ± 6.11
	K_{A3}	-27.8 ± 3.46	0.52 ± 3.39	-27.3 ± 6.85
TOCDL	K_{A1}	-34.5 ± 1.97	5.52 ± 1.93	-29.0 ± 3.90
	K_{A2}	-38.4 ± 2.46	10.6 ± 2.40	-27.9 ± 4.86
	K_{A3}	-41.6 ± 3.64	14.2 ± 3.57	-27.5 ± 7.21
DLPG	K_{A1}	-45.6 ± 3.76	16.6 ± 3.69	-29.0 ± 7.45
	K_{A2}	-45.7 ± 3.60	17.7 ± 3.52	-28.0 ± 7.12
	K_{A3}	-51.5 ± 2.27	23.9 ± 2.23	-27.6 ± 4.50
DMPG	K_{A1}	-40.1 ± 4.36	11.0 ± 4.29	-29.2 ± 8.65
	K_{A2}	-40.9 ± 1.91	12.8 ± 1.88	-28.1 ± 3.79
	K_{A3}	-39.6 ± 4.85	11.9 ± 4.76	-27.7 ± 9.61
DPPG	K_{A1}	-24.5 ± 2.59	-2.80 ± 2.53	-27.3 ± 5.12
	K_{A2}	-28.5 ± 4.32	2.30 ± 4.24	-26.2 ± 8.56
	K_{A3}	-28.3 ± 3.25	2.55 ± 3.17	-25.7 ± 6.42

Table S6. Binding affinities for AmtB^{N72AN79A}-lipid binding. Reported as described in Table S1.

Lipid	T (K)	K_{D1} (μM)	K_{D2} (μM)	K_{D3} (μM)	R^2	χ^2
POPG	298	10.7 ± 3.84	16.0 ± 7.19	19.4 ± 8.10	0.99	0.014
	302	11.7 ± 3.75	18.5 ± 7.12	22.2 ± 8.30	0.99	0.014
	306	13.1 ± 2.75	20.5 ± 4.75	24.9 ± 6.82	0.99	0.015
	310	15.0 ± 3.35	24.3 ± 7.12	30.7 ± 11.8	0.99	0.012
POPE	298	9.23 ± 2.81	13.5 ± 4.60	15.2 ± 5.24	0.99	0.023
	302	11.3 ± 1.68	16.3 ± 2.85	19.0 ± 4.25	0.99	0.021
	306	12.6 ± 2.05	17.7 ± 3.01	20.8 ± 4.64	0.99	0.015
	310	15.1 ± 3.27	22.9 ± 4.60	26.1 ± 7.93	0.99	0.013

Table S7. Thermodynamic parameters for AmtB^{N72AN79A}-lipid binding. Reported as described in Table S3.

Lipid		ΔH (kJ/mol)	-TΔS (298K) (kJ/mol)	ΔG (298K) (kJ/mol)
POPG	K_{A1}	-23.5 ± 0.76	-5.00 ± 0.74	-28.5 ± 1.50
	K_{A2}	-29.5 ± 0.96	1.88 ± 0.90	-27.6 ± 1.86
	K_{A3}	-29.0 ± 1.24	1.91 ± 1.20	-27.1 ± 2.44
POPE	K_{A1}	-31.7 ± 3.08	2.90 ± 3.02	-28.8 ± 6.10
	K_{A2}	-33.9 ± 4.46	6.00 ± 4.39	-27.9 ± 8.85
	K_{A3}	-33.4 ± 3.88	5.85 ± 3.80	-27.6 ± 7.68

Supplementary References

(1) Laganowsky, A.; Reading, E.; Allison, T. M.; Ulmschneider, M. B.; Degiacomi, M. T.; Baldwin, A. J.; Robinson, C. V. *Nature* **2014**, *510*, 172.

(2) Laganowsky, A.; Reading, E.; Hopper, J. T.; Robinson, C. V. *Nat. Protoc.* **2013**, *8*, 639.

(3) Subbarow, C. H. F. a. Y. *J. Biol. Chem.* **1925**, *66*, 26.

(4) P. S. Chen, T. Y. T., Huber Warner *Anal. Chem.* **1956**, *28*, 3.

(5) Allison, T. M.; Reading, E.; Liko, I.; Baldwin, A. J.; Laganowsky, A.; Robinson, C. V. *Nat. Commun.* **2015**, *6*, 8551.

(6) Marty, M. T.; Baldwin, A. J.; Marklund, E. G.; Hochberg, G. K.; Benesch, J. L.; Robinson, C. V. *Anal. Chem.* **2015**, *87*, 4370.

(7) Stengel, F.; Baldwin, A. J.; Bush, M. F.; Hilton, G. R.; Lioe, H.; Basha, E.; Jaya, N.; Vierling, E.; Benesch, J. L. *Chem. Biol.* **2012**, *19*, 599.

(8) van't Hoff, M. J. H. *Recl. Trav. Chim. Pays-Bas* **1884**, *3*, 333.